NUMERICAL EXPERIMENT ON VARIANCE BIASES AND MONTE CARLO NEUTRONICS ANALYSIS WITH THERMAL HYDRAULIC FEEDBACK

Hyung Jin Shim, Beom Seok Han, and Chang Hyo Kim
Nuclear Engineering Department
Seoul National University, Seoul, Korea
shj@wooritg.com; beomseok@snu.ac.kr; kchyo@snu.ac.kr

Abstract

Monte Carlo (MC) power method based on the fixed number of fission sites at the beginning of each cycle is known to cause biases in the variances of the k-eigenvalue (k_{eff}) and the fission reaction rate estimates. Because of the biases, the apparent variances of k_{eff} and the fission reaction rate estimates from a single MC run tend to be smaller or larger than the real variances of the corresponding quantities, depending on the degree of the inter-generational correlation of the sample. We demonstrate this through a numerical experiment involving 100 independent MC runs for the neutronics analysis of a 17x17 fuel assembly of a pressurized water reactor (PWR). We also demonstrate through the numerical experiment that Gelbard and Prael's batch method and Ueki et al's covariance estimation method enable one to estimate the approximate real variances of k_{eff} and the fission reaction rate estimates from a single MC run. We then show that the use of the approximate real variances from the two-bias predicting methods instead of the apparent variances provides an efficient MC power iteration scheme that is required in the MC neutronics analysis of a real system to determine the pin power distribution consistent with the thermal hydraulic (TH) conditions of individual pins of the system.

Key Words: MC power method, batch method, covariance estimation method, apparent variances, real variances, k_{eff} bias.

Introduction

Monte Carlo power method based on the cycle-by-cycle eigenvalue estimates with the fixed number of fission sites at the beginning of each cycle results in biases in the variances of the k-eigenvalue (k_{eff} hereafter) and the fission reaction estimates [1-7] due to inter-generational correlation of the fission sites. As a result, the apparent variances of k_{eff} and the fission reaction rate estimates from a single Monte Carlo (MC) run tend to be smaller or larger than the real variances of the corresponding parameters and thus the standard errors of the MC estimates on these parameters are apt to be underestimated or overestimated in comparison with the real ones. We observe that the use of the apparent variances smaller than the real variances may cause inefficiency in the iterative MC power distribution calculations which are required in neutronics analysis of a real reactor system to determine the pin power distribution consistent with the thermal hydraulic (TH) conditions of individual pins comprising the reactor system.

In this paper we will show that one can avoid the inefficiency of the iterative MC calculations with T/H feedback taken into account by using the approximate real variances estimated by bias-predicting methods instead of the apparent variances. We will present first a comparison of the two bias-predicting methods; Gelbard and Prael's batch method [4] and Ueki et al's intercycle covariance estimation method (covariance method hereafter) [8], through a numerical experiment on variance biases in the neutronics analysis of a real 17x17 PWR fuel assembly and discuss how good they are in obtaining the approximate real variances. Then we will use the approximate real variances to devise an efficient MC power iteration scheme that may require the shortest possible computing time in obtaining the pin power distribution consistent with the T/H condition.

Numerical Experiment on Variance Biases

It is well known that the MC eigenvalue calculations based on power iteration methods are biased [1-7]. There are various methods designed either to determine or to reduce the biases. We observe that the batch method and the covariance method are easier to implement in our Monte Carlo neutronics code, MCCARD [9]. But we note that the performance of these methods have been tested for rather simplified neutronics problems instead of the real neutronics problems. In case of Ueki et al's method, it is tested for the k_{eff} bias estimate only, even though it can also be applicable to the power density biases. To make comparison of the effectiveness of the two methods, we perform here continuous energy MC k_{eff} and pin power distribution calculations for the 17x17 Type-A FA of the small pressurized water reactor, SMART, in Figure 1A on the octant symmetry using the MC-CARD code.

To estimate the real variances of the k_{eff} and individual pin power densities, we conduct 100 independent MC runs with each MC run based on 25,000 particle histories per cycle on 700 cycles including 200 settling cycles. The real and apparent variances of either k_{eff} or individual pin power densities are estimated by

$$s_R^2 \approx \frac{1}{\text{M-1}} \sum_{i=1}^{M} \left(\frac{1}{N} \sum_{j=1}^{N} q_j^i - \frac{1}{M} \sum_{i=1}^{M} \frac{1}{N} \sum_{j=1}^{N} q_j^i \right)^2 \quad (1)$$

and

$$s_A^2 = \frac{1}{M} \sum_{i=1}^{M} \frac{1}{N(N-1)} \sum_{j=1}^{N} \left(q_j^i - \frac{1}{N} \sum_{m=1}^{N} q_m^i \right)^2 \quad (2)$$

where M denotes the number of the independent MC replicas and q_j^i denotes the MC estimates of either k_{eff} or pin power densities at the cycle j in the i^{th} MC run. The apparent variances as well as approximate real variances from a single MC run by the two bias-predicting methods are compared with the estimated real variances from 100 MC runs.

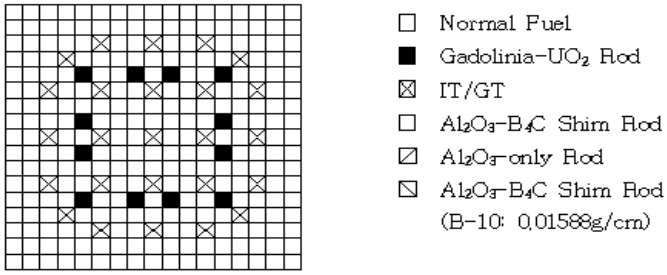

Figure 1A. Layout and Composition of the Type-A Fuel Assembly

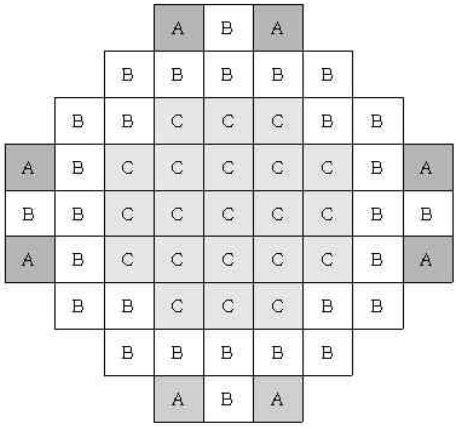

Type	No.	Normal Rods	Gd Rods	B-10 (g/cm)	Al_2O_3-B_4C Rods	Axial Zonning
A	8	224	12	0.01110	28	28 / 0
B	28	240	4	0.01588	20	16 / 4
C	21	236	4	0.01588 0.02900	8 16	8 / 0 8 / 8
Total	57	13,468	292	-	1,288	-

*Axial Zonning : Al_2O_3-B_4C / Al_2O_3-only

Figure 1B. Layout and Composition of the SMART Core

Table 1 shows the k_{eff} estimate of the FA and the associated real variance, s_R^2, from Eq. (1). $s_{R,est}^2$ stands for the approximate real variance of k_{eff} estimated either by the batch method or by the covariance method. The three most common k_{eff} estimators such as collision estimator, absorption estimator and the track-length estimator give practically the same estimates on k_{eff}, reflecting that they are unbiased estimators. The apparent variance of k_{eff} by a single MC run is shown to underestimate the real variance, particularly in the collision and absorption estimates for k_{eff}. The batch method and the covariance method predict the approximate real variance in

good agreement with the real variance. The larger the batch size, the better the approximate real variances. In case of the covariance method, the results in Table 1 indicate that the approximate real variance estimated with the correlation length of 20 is the closest to the real k_{eff} variance.

Table 1. Comparison of two bias-predicting methods for variance estimation of k_{eff}

k_{eff} Estimator / Sample Variance Estimate Method		Collision Estimator			
		k_{eff}	s_R	$s_{R,est}$	$s_R^2/s_{R,est}^2$
No Correlation		0.99824	2.80E-04	2.20E-04	1.27
Gelbard's Method	10 cycles/batch			2.30E-04	1.22
	20 cycles/batch			2.37E-04	1.18
	50 cycles/batch			2.41E-04	1.16
Ueki's Method	10 lag covariance			2.39E-04	1.17
	20 lag covariance			2.46E-04	1.14
	50 lag covariance			2.41E-04	1.16
k_{eff} Estimator / Sample Variance Estimate Method		Absorption Estimator			
		k_{eff}	s_R	$s_{R,est}$	$s_R^2/s_{R,est}^2$
No Correlation		0.99823	2.40E-04	2.16E-04	1.11
Gelbard's Method	10 cycles/batch			2.22E-04	1.08
	20 cycles/batch			2.22E-04	1.08
	50 cycles/batch			2.24E-04	1.07
Ueki's Method	10 lag covariance			2.29E-04	1.05
	20 lag covariance			2.26E-04	1.06
	50 lag covariance			2.42E-04	0.99
k_{eff} Estimator / Sample Variance Estimate Method		Track Length Estimator			
		k_{eff}	s_R	$s_{R,est}$	$s_R^2/s_{R,est}^2$
No Correlation		0.99823	3.00E-04	2.86E-04	1.05
Gelbard's Method	10 cycles/batch			2.88E-04	1.04
	20 cycles/batch			2.91E-04	1.03
	50 cycles/batch			2.94E-04	1.02
Ueki's Method	10 lag covariance			2.86E-04	1.05
	20 lag covariance			2.91E-04	1.03
	50 lag covariance			3.19E-04	0.94

Figures 2A to 2C show a comparison of estimaties on individual pin power densities and the associated variances. Like the case of k_{eff} estimate, the apparent variances from a single MC run underestimate the real variances of the pin power estimates. In contrast to the case of k_{eff} estimate, however, the difference between the real and apparent variances of the individual pin power density estimates is observed to be much larger than that of k_{eff}. In several fuel pins, the apparent variances are observed less than half of their real variances. Results in these figures

show that both the batch method and the covariance method can produce approximate but fairly good estimates for the real variances of pin power density estimates. The larger the batch size or the correlation length is, the better the approximate real variances of individual pin power densities result from the batch method or covariance method.

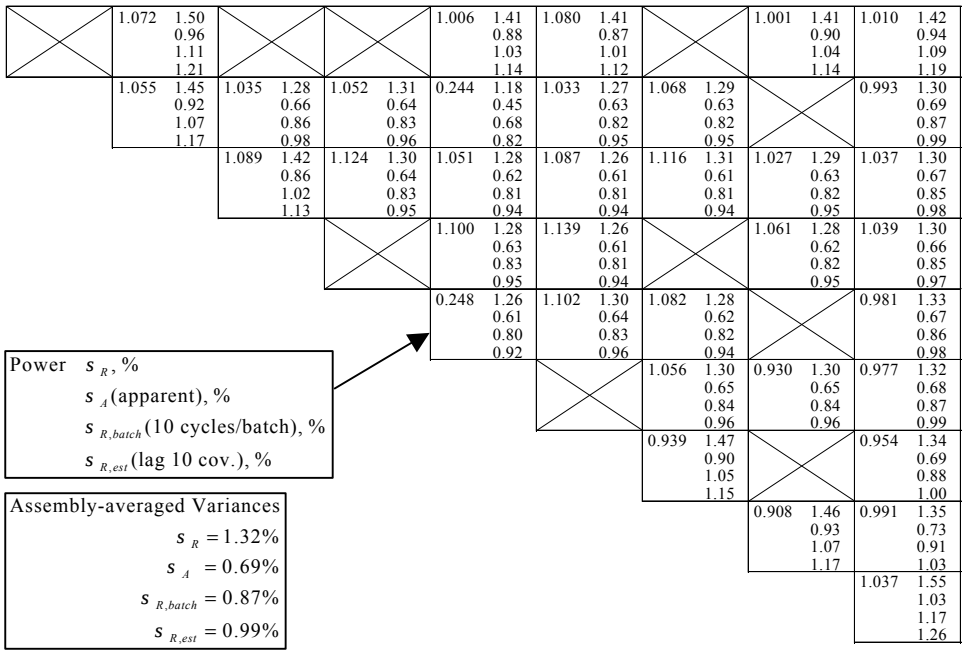

Figure 2A. Comparison of Variance Estimations on Normalized Pin Power Densities (The case of 10 inter-cycle correlations or 10 batch size)

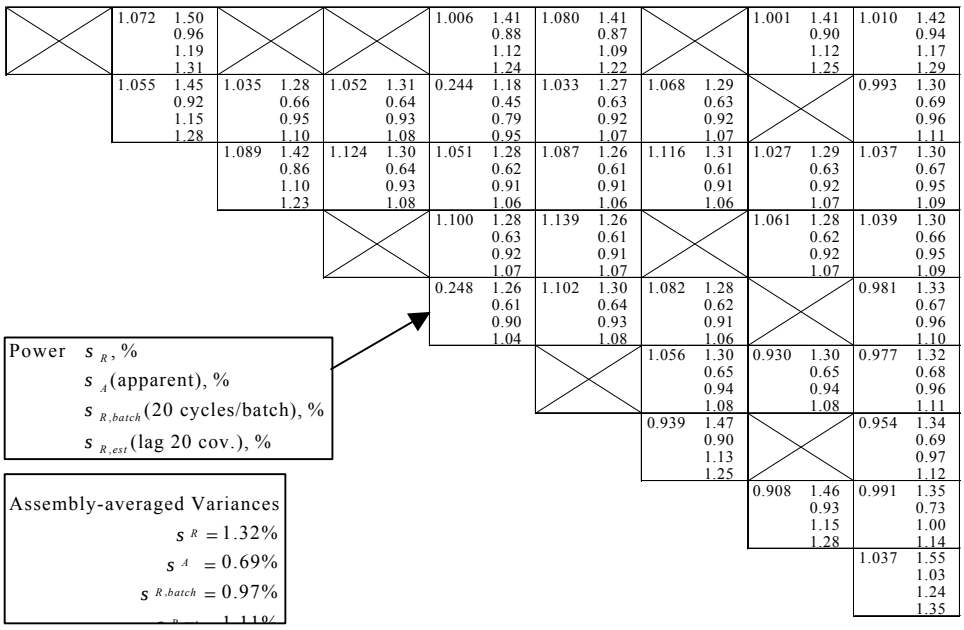

Figure 2B. Comparison of Variance Estimations on Normalized Pin Power Densities (the case of 20 inter-cycle correlations or 20 batch size)

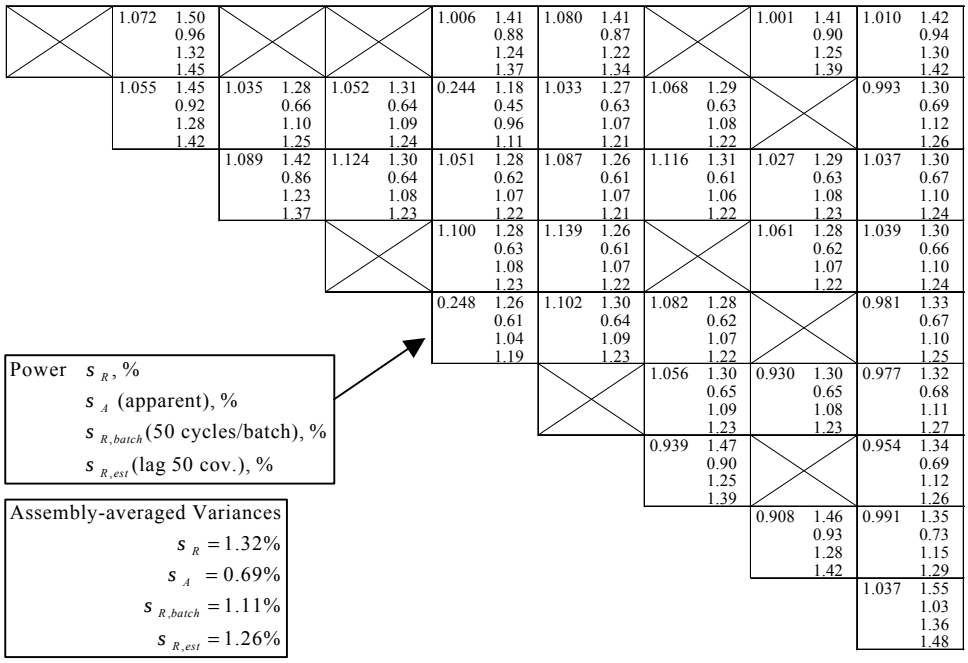

Figure 2C. Comparison of Variance Estimations on Normalized Pin Power Densities (The case of 50 inter-cycle correlations or 50 batch size)

MC Neutronics Calculations with T/H Feedback

The neutronics analysis of a real reactor system generally requires repeating the neutronics calculations several times until the resulting power distribution as well as k_{eff} matches the T/H condition of the system. Because even a single MC run for the power distribution calculation is very time-consuming, it is desirable to devise an efficient MC iterative scheme that can reduce the computational time required for the repeated MC neutronics calculations. In this section, we will demonstrate that one can devise an efficient MC power iteration scheme by utilizing the standard error, i.e., the square root of the approximate real variance, as a convergence criterion for the pin power distribution.

Figure 3 displays an iterative MC power calculation flowchart. It is similar to the one adopted by the deterministic neutronics codes but differs from them in that the whole MC iteration process is divided into two stages: I and II. The stage I MC iterations are designed to determine the T/H condition that matches the power distribution of the system as quickly as possible using rather coarse MC power distribution calculations. The MC power distribution calculations in stage I are performed by generating the smaller number of particle histories than more refined stage II MC calculations either by taking the number of particle histories per cycle or the total number of cycles per MC run as small as possible. The resulting coarse MC power distribution is used to determine the intermediate T/H condition, which in turn is used for the MC power distribution calculation in the subsequent MC iteration. When the difference between the T/H conditions of two consecutive MC iterations satisfies the preset convergence criterion

on the T/H condition, the stage II MC iteration is switched on for more refined MC power distribution calculation and the T/H calculation in turn.

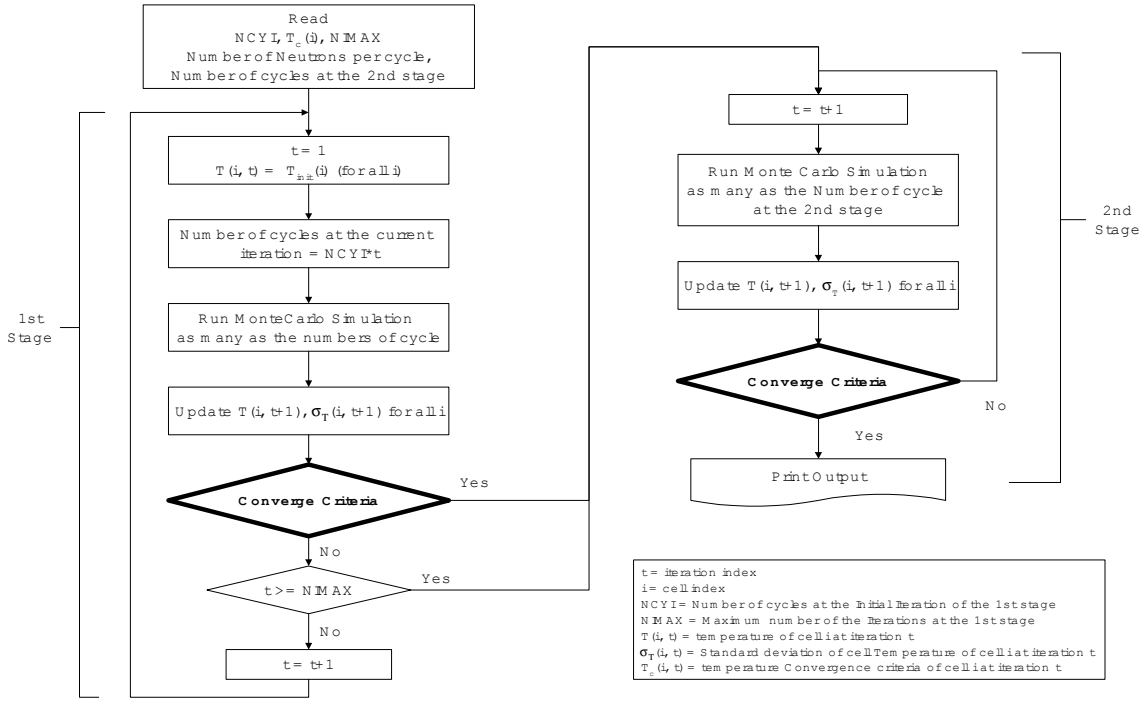

Figure 3. Flowchart of Iterative MC Neutronics Calculation with Thermal Hydraulic Feedback

The stage I and II MC iterations are characterized by such parameters as the number of neutron histories per cycle (NNHC), the number of cycles at the initial iteration (NCYI) at the stage I, and the number of cycles per MC run (NCYL). These parameters determine the computational condition of the MC calculations and affect the convergence of T/H condition and the MC computing time as well. The NCYL in the stage I starts with NCYI and increases as iterations progress with increasing iteration index i by i times NCYI. The MC power distribution and the T/H condition from the earlier MC iterations before the final convergence are intermediate results. Thus the stage I iteration scheme is devised in such a way that one spends less computing time for determining the intermediate results on the MC power and the T/H conditions at the earlier iterations than the computing time for determining the converged results at the later iterations. The stage II iteration is designed not only to confirm whether the converged T/H condition from the stage I matches the power distribution from more refined MC calculation but to obtain the T/H condition consistent with the power distribution from refined MC calculations. Unlike the case of the stage I, therefore, the NCYL at the stage II is set fixed so that the MC power distribution as well as the multiplication factor are determined with acceptable standard deviation.

The bold-framed diamond in Figure 3 specifies the convergence criteria. We tested three different criteria:

(.) $\max\left|T_l^{i+1} - T_l^i\right| \le \Delta T$

(.) $\max\left|T_l^{i+1} - T_l^i\right| \le \Delta T$ or $\max\left|T_l^{i+1} - T_l^i\right| \le a s_A$

(.) $\max\left|T_l^{i+1} - T_l^i\right| \le \Delta T$ or $\max\left|T_l^{i+1} - T_l^i\right| \le a s_{R,est}$

T_l^k (k=i or i+1) is the temperature of the cell l at the k^{th} MC run. The criterion I terminates the iterative MC runs when the maximum cell temperature difference between two consecutive MC runs is less than the set value ΔT. Note that this is the criterion adopted by most of the deterministic codes. Because of the standard errors associated with T_l^k (k=i or i+1), the criteria II and III are designed to account for them. These two criteria terminate the MC iteration when the maximum cell temperature difference between two consecutive MC runs is less than ΔT or less than a times the standard error s_A (case II) or $s_{R,est}$ (case III) of T_l^{i+1}. a here determines the confidence level of T_l^{i+1} estimate determined from MC pin power distribution and are chosen 3 here.

The effectiveness of the three convergence criteria for the iterative MC scheme in Figure 3 is examined by the MCCARD analysis for the 17x17 Type-A FA and SMART core. The T/H conditions of the FA are specified by the temperatures of the fuel pellet and cladding of each radial and axial fuel pin segment, and water coolant temperature along each coolant channel. The temperature convergence limits on the fuel cells and the water coolant cells are set as $\Delta T(\text{fuel}) \le 5^oK$ and $\Delta T(\text{coolant}) \le 2^oK$, respectively. Figure 4 shows the T/H convergence characteristics of the iterative MC calculations in terms of the maximum fuel cell temperature difference between two consecutive MC iterations as a function of iteration index. It is noted that the convergence criterion I requires the most MC iterations, while the convergence criterion III the least MC iterations, to produce the MC pin power distribution consistent with the T/H condition within the preset criteria. The error bars attached at the end of each iteration scheme denote $3 s_{R,est}$ of the limiting fuel cell temperature exhibiting the maximum $\Delta T(\text{fuel})$. Note that $\pm 3 s_{R,est}$ correspond to the 99.7 % confidence range that the true mean fuel temperature lies about the estimated fuel cell temperature. Therefore, once the temperature estimate of the limiting fuel cell comes in this range, it may be in vain to continue the MC iterations in order to reduce the maximum $\Delta T(\text{fuel})$ further. For 99.7 % of the new temperature estimates from the continued MC power iteration remains in this range and consequently the maximum $\Delta T(\text{fuel})$ may either fluctuate or show very slow convergence since then. This is clearly noted in the MC iterations based on the convergence criterion I in Figure 4. The convergence criterion II terminates the MC iterations earlier than the convergence criterion I. Because the apparent variances underestimate the real variances and the standard errors accordingly, however, the convergence criterion II still causes more MC iterations than are necessary as demonstrated in the case with convergence criterion III.

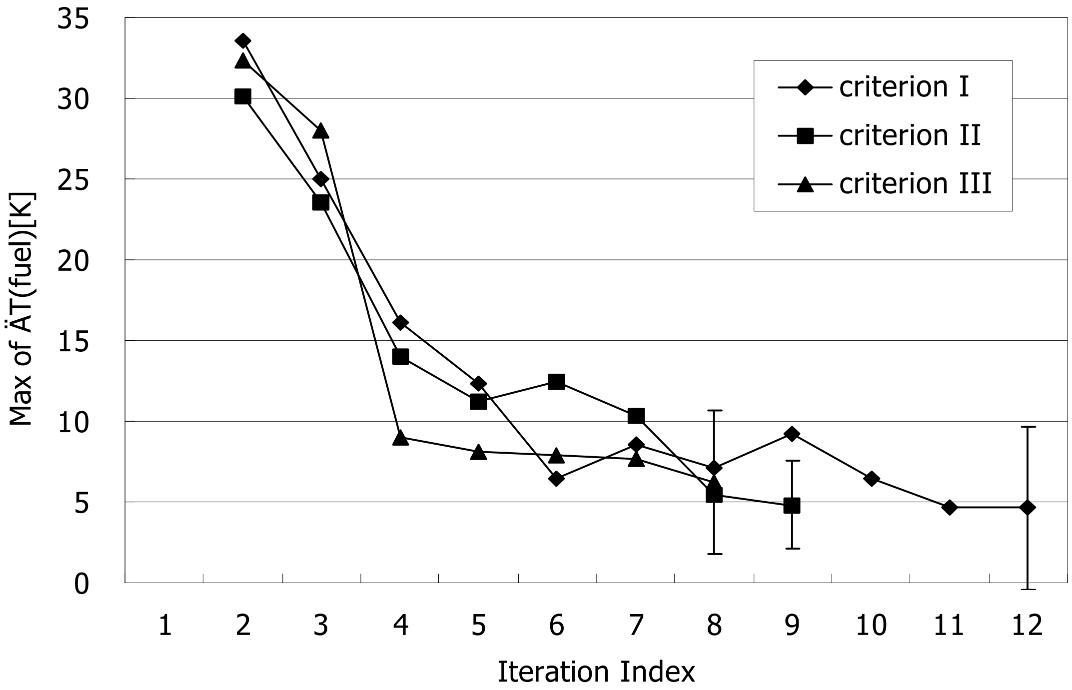

Figure 4. Convergence Characteristics of the Fuel Temperatures for the

Figure 5 shows a comparison of the radial pin power distributions from iterative MC calculations based on the convergence criteria I and III. It is observed that two convergence criteria affect a lot the total number of the required MC iterations but that they do not have any noticeable effect on the results of the converged power distributions.

	1.074 0.009 1.071 0.008 -0.26			1.007 0.008 1.006 0.007 -0.03	1.081 0.009 1.082 0.008 0.09		1.002 0.008 1.003 0.007 0.16	1.010 0.009 1.009 0.008 -0.16
	1.052 0.009 1.054 0.007 0.14	1.036 0.008 1.034 0.006 -0.12	1.052 0.007 1.052 0.007 0.01	0.245 0.001 0.245 0.001 -0.02	1.034 0.007 1.032 0.006 -0.13	1.068 0.008 1.068 0.006 -0.02		0.993 0.008 0.995 0.006 0.20
		1.089 0.010 1.087 0.007 -0.16	1.126 0.009 1.126 0.006 0.04	1.050 0.009 1.050 0.006 0.02	1.088 0.009 1.085 0.007 -0.27	1.117 0.009 1.116 0.007 -0.07	1.027 0.008 1.026 0.006 -0.11	1.036 0.009 1.037 0.006 0.09
				1.097 0.008 1.099 0.006 0.16	1.138 0.009 1.139 0.007 0.08		1.061 0.008 1.061 0.006 0.06	1.039 0.009 1.040 0.006 0.11
				0.248 0.001 0.248 0.001 0.05	1.100 0.009 1.100 0.006 0.04	1.083 0.008 1.085 0.006 0.16		0.980 0.008 0.979 0.007 -0.11
						1.055 0.009 1.056 0.007 0.13	0.931 0.007 0.929 0.006 -0.24	0.976 0.008 0.977 0.006 0.13
						0.940 0.008 0.940 0.006 0.02		0.953 0.007 0.955 0.006 0.20
							0.908 0.007 0.908 0.006 -0.03	0.992 0.007 0.990 0.006 -0.20
								1.038 0.010 1.037 0.008 -0.14

* Power(A) : Pin Power Density[criterion I]
Power(B) : Pin Power Density[criterion III]
Relative Error(%) = (B-A)/A*100

Figure 5. Comparison of Normalized Pin Power Distributions for the Fuel

For further examination of the effectiveness of the convergence criteria, the MC core neutronics calculations with T/H feedback are performed to determine the core multiplication factor (k_{eff}) and the fuel pin and fuel assembly normalized power distributions in SMART PWR in the hot full power (HFP) condition at the beginning of its life. The core MC calculation is conducted on the octant symmetry, employing 100,000 particle histories per cycle with 100 cycles for NCYI and 1,000 cycles for NCYL of the second stage MC iterations. The reactor is axially divided into 15 segments in which 10 equal-length segments account for the active core height, and 3 segments at the top and 2 segments at the bottom of the core represent the top and bottom reflectors. The pellet, gap, and cladding associated with each fuel pin are treated as individual computational cells. For simplicity of T/H calculation and consideration of the computer memory, the water coolant in each axial segment of a fuel assembly is treated as a single computational cell. This division of the reactor leads to a total of 35,330 MC computational cells. Figure 6 shows the fuel temperature convergence characteristics of the iterative MC calculations for the SMART core. As observed already in the FA analysis, the criterion III allows one to avoid the unnecessary MC iteration and thus enhance the efficiency of the iterative MC calculations significantly. Figures 7A to 7B show the normalized assembly power distributions and the radial pin power peaking factors of the individual FA's, respectively, in the SMART core from two MC calculations with two different convergence criteria I and III. The determination of the pin and FA power distribution from the criterion III required the smaller number of MC iterations than that from the criterion I. But the power distributions from the two MC calculations are strikingly similar to each other.

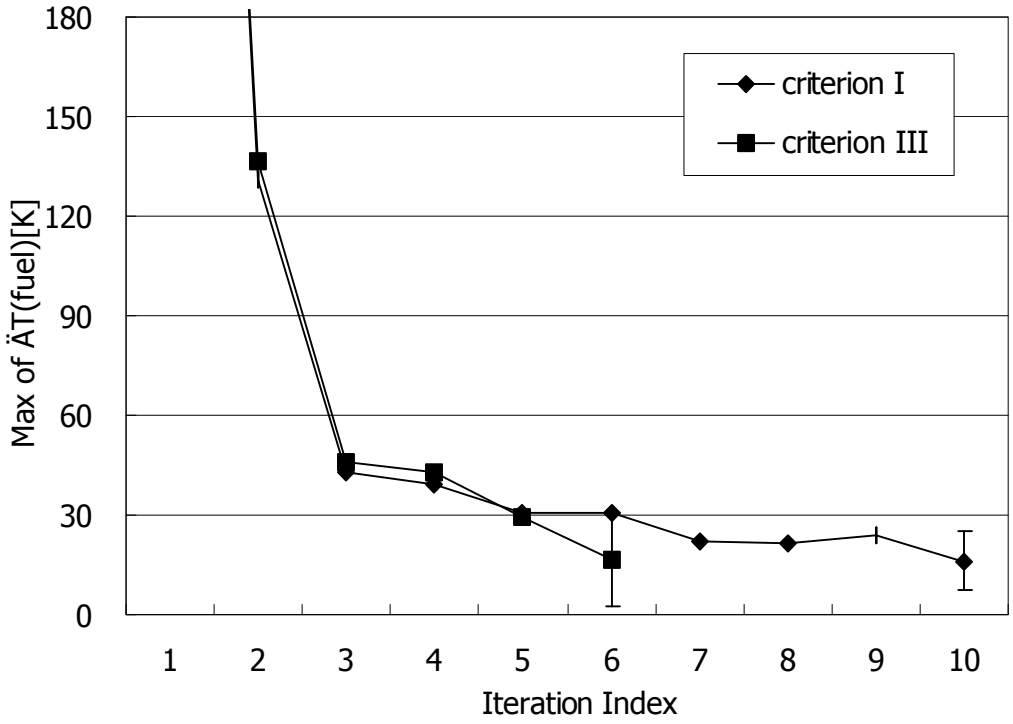

Figure 6. Convergence Characteristics of the Fuel Temperatures for the SMART Core.

1.547	0.013	1.489	0.012	1.343	0.011	1.118	0.011	0.586	0.008
1.536	0.015	1.478	0.013	1.336	0.012	1.117	0.011	0.593	0.008
-0.688		-0.696		-0.546		-0.021		1.163	
		1.438	0.012	1.278	0.011	1.002	0.010	0.402	0.006
		1.427	0.013	1.271	0.011	1.004	0.010	0.410	0.006
		-0.699		-0.547		0.250		1.848	
Pow(A)	s_A			1.135	0.011	0.695	0.008		
Pow(B)	$s_{R,est}$			1.136	0.011	0.704	0.008		
Error(%)				0.023		1.269			

* Pow(A) : Assemblywise Power Density[criterion I]
  Pow(B) : Assemblywise Power Density[criterion III]
  Error(%)=(B-A)/A*100

Figure 7A. Normalized Fuel Assembly Power Distribution for the SMART Core.

1.714	0.016	1.703	0.020	1.576	0.020	1.358	0.019	0.884	0.015
1.701	0.022	1.688	0.022	1.567	0.021	1.372	0.019	0.896	0.016
-0.745		-0.887		-0.548		1.004		1.338	
		1.649	0.015	1.511	0.014	1.251	0.013	0.775	0.010
		1.643	0.016	1.508	0.014	1.248	0.013	0.781	0.011
		-0.363		-0.212		-0.214		0.671	
Pow(A)	s_A			1.366	0.014	1.069	0.012		
Pow(B)	$s_{R,est}$			1.356	0.014	1.070	0.012		
Error(%)				-0.718		0.080			

* Pow(A) : Maximum Pin Power Density[criterion I]
  Pow(B) : Maximum Pin Power Density[criterion III]
  Error(%)=(B-A)/A*100

Figure 7B. Assemblywise Pin Peaking Factor for the SMART Core.

Summary

The neutronics analysis of the real reactor system by the deterministic or the stochastic method requires the iterative power distribution and T/H calculations in order to determine the power distribution consistent with the T/H condition of the system. Because even a single MC power calculation costs the excessive computing time, the iterative MC computational scheme along with the power and T/H convergence criteria need be designed toward the maximum efficiency. As a way to attain the desired efficiency, we devised a MC power and T/H iteration scheme along with the convergence criteria including the standard errors of the MC pin power estimates. We demonstrated the efficiency of the iterative MC calculation scheme in terms of neutronics analysis of the real reactor system. We also demonstrated the importance of correcting the variance biases of the pin power density estimates ae well as the keff estimates

from a single MC run in attaining the desired efficiency of the MC power iteration. The MC neutronics calculations have not been mature enough for the reactor designers to adopt the MC power and T/H iterations. With the ever-advancing computer technology in terms of memory, speed, networking and parallel computing, however, the results in this paper will be useful for the real reactor problems that may call for MC nuclear analysis.

References

1. H. Bowsher, E.M. Gelbard, P. Gemmel, G. Park, ”Magnitude of Bias in Monte Carlo Eigenvalue Calculations,” *Trans. Am. Nucl. Soc.*, 45, 324 (1983).
2. V.G. Zolotukhin and L.V. Maiorov, “An Estimate of the Systematic Errors in the calculation of criticality by the Monte Carlo Method,” *Atomnaya Energiya*, 55, 3, PP173-175(Sep. 1983).
3. R. J. Brissenden and A. R. Garlick, “Biases in the Estimation of Keff and its Error by Monte Carlo Methods,” *Ann. Nucl. Energy*, 13, 63 (1986).
4. E. M. Gelbard and R. Prael, “Computation of Standard Deviations in Eigenvalue Calculations,” *Prog. Nucl. Energy*, 24, 237 (1990).
5. Ely M. Gelbard, ”Monte Carlo Eigenvalue Biases: Generalization Beyond the Absorption Estimate,” *Trans. Am. Nucl. Soc.*, 64, 302 (1991).
6. E. M. Gelbard and Albert G. Gu, “Biases in Monte Carlo Eigenvalue Calculations,” *Nucl. Sci. Eng.*, 117,1-9(1994).
7. R. N. Blomquist and E. M. Gelbard, “Alternative Implementations of the Monte Carlo Power Method,” *Nucl. Sci. Eng.*, 141, 85-100 (2002).
8. Taro Ueki, Takamasa Mori, and Massayuki Nakagawa, “Error Estimation and their Biases in Monte Carlo Eigenvalue Calculations,” *Nucl. Sci. Eng.*, 125, 1-11 (1997).
9. Hyung Jin Shim and Chang Hyo Kim,”Error Propagation Module Implemented in MC-CARD Monte Carlo Code,” *Trans. Am. Nucl. Soc.*, 86, 325 (2002).